Subsonic Axisymmetric Near-Wake Studies

R. A. Merz*
Air Force Institute of Technology, Wright-Patterson Air Force Base, Ohio
and
R. H. Page† and C. E. G. Przirembel‡
Rutgers University, New Brunswick, N.J.

The turbulent near-wake of a cylindrical blunt-based body aligned with a uniform freestream was experimentally investigated. Tests were conducted over the entire subsonic Mach number range in a wind tunnel utilizing an upstream model support system. Results indicate that the separation process influences the flow approaching the blunt base for at least 3 model diameters. The base pressure coefficient is constant for Mach numbers less than 0.8, but drops rapidly at near-sonic speeds. The size of the near-wake increases with Mach number. A similarity expression for the near-wake centerline velocity distribution is developed.

Nomenclature

C_p = pressure coefficient, $=2(P-P_\infty)/\rho U_\infty^2$
C_{pb} = base pressure coefficient
H = boundary-layer shape factor, $=\delta_1/\delta_2$
D = model diameter
M = Mach number
M_1 = reference Mach number at $x/D=-3.0$
M_c = near-wake centerline Mach number
ΔM = change in Mach number $M_L - M_\infty$
N = power law exponent
P = pressure
P_b = base pressure
r = radial distance from model centerline
R_0 = model radius
U = velocity
U_{max} = maximum velocity
U_c = near-wake centerline velocity
U_{cmax} = maximum near-wake centerline velocity
x = axial distance from base (positive: downstream, negative: upstream)
$x_{s.p.}$ = location of rear stagnation point
Y = radial distance from model wall
δ = boundary-layer thickness
δ_1 = boundary-layer displacement thickness
δ_2 = boundary-layer momentum thickness
ρ = density

Subscripts

∞ = freestream condition
L = local condition
atm = ambient atmospheric condition

Introduction

THE abrupt change in the rear geometry of a bluff body moving through a real fluid causes the external flow to separate from the body. This separated region, which occurs at or near the base of the body, is usually referred to as the near-wake of the body. The near-wake is dominated by the mixing process associated with the free shear layer that results from the flow separation. While not large, this zone has a significant influence on base drag, base heat transfer, and the configuration of the far-wake. The components that comprise the near-wake flowfield of a blunt axisymmetric body are shown in Fig. 1.

The subsonic base flow problem has been the subject of a great deal of study in recent years. References 1-19 represent only a small portion of the numerous experimental investigation of the phenomenon. Rather complete reviews of the available literature may be found in Refs. 20-22.

One of the most common near-wake parameters reported in the literature is base pressure. Figure 2 represents a compilation of some of the available data and shows base pressure coefficient plotted against Mach number. These data have been obtained for a wide variety of model geometries, with varying approach flow conditions and in numerous facilities both with and without support interference. From the scatter in these data, it can be seen that there was a need for a systematic study of the turbulent near-wake of a simple axisymmetric blunt body in one test facility over the entire subsonic speed range.

In view of this apparent need, a comprehensive experimental investigation was carried out. The present results represent the first detailed investigation of the near-wake of a single, simple geometric shape (i.e., the axisymmetric blunt base of a right circular cylinder aligned with the flow direction—Fig. 1), in a single test facility free from model support interference over the entire subsonic speed range.

Experimental Apparatus and Technique

This experimental investigation was conducted in a second generation Rutgers Axisymmetric Near-Wake Tunnel (RANT II). This tunnel is an open jet, blow-down type facility capable of producing speeds over the entire subsonic Mach number range. RANT II was designed and constructed for interference-free studies of turbulent axisymmetric near-wakes at subsonic speeds. As shown in Fig. 3, the unique feature of RANT II is an upstream sting that was designed as an integral part of the nozzle to produce uniform flow over a 1.9 cm diam cylindrical model. The nozzle has an overall contraction ratio of 8:1 and an exit diameter of 10.16 cm. A more complete description of the facility may be found in Ref. 20.

Preliminary measurements were made to insure that the tunnel produced a satisfactory flowfield for the present investigation. For these measurements, the centerbody was extended over 6 model diameters downstream of the nozzle

Presented as Paper 77-135 at the AIAA 15th Aerospace Sciences Meeting, Los Angeles, Calif., Jan. 24-26, 1977; submitted Feb. 1, 1977; revision received March 27, 1978.

Index categories: Jets, Wakes, and Viscid-Inviscid Flow Interactions; Viscous Nonboundary-Layer Flows; Subsonic Flow.

*Assistant Professor, Department of Aeronautics and Astronautics. Member AIAA.

†Professor, Mechanical, Industrial, and Aerospace Engineering Department. Associate Fellow AIAA.

‡Associate Professor, Mechanical, Industrial, and Aerospace Engineering Department. Associate Fellow AIAA.

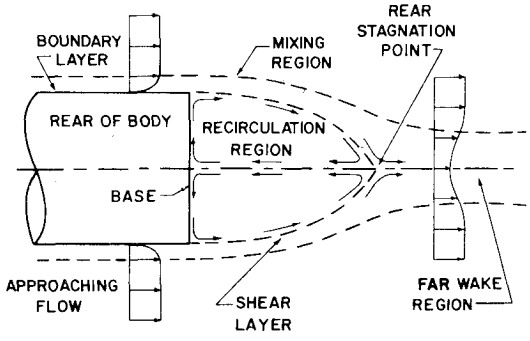

Fig. 1 Flowfield schematic.

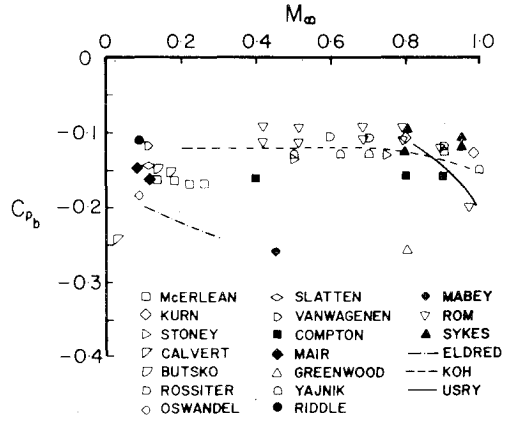

Fig. 2 Summary of available base pressure data.

exit. With the centerbody extended, it was possible to measure the flow characteristics of the tunnel without any influence of the blunt base on the flowfield. Total and static pressures were measured throughout the flowfield using a standard Prandtl pitot-static probe. In addition, the static pressures at various axial locations on the nozzle wall and centerbody were measured. These results showed that: 1) the freestream was uniform and axisymmetric to within 0.5% of the freestream velocity at all Mach numbers; 2) at all speeds, the Mach number was constant in the axial direction to within 1% for a distance of ±4 model diam of the nozzle exit; and 3) the core region of the free jet extended over 20 model diameters downstream of the blunt base and was of sufficient size so that meaningful near-wake measurements could be made. In addition, similar measurements with the blunt base, just upstream of the nozzle exit (Fig. 3), showed that the nozzle flowfield had not been altered by the blunt base.

The boundary layer on the model was measured at three axial locations upstream of the base. These measurements were made at 1, 2, and 4 model diameters upstream of the base with a model that incorporated a total pressure rake in its design. The rake model contained nine total pressure probes that protruded from the model surface. The probes were equally spaced around the model circumference at 40 deg intervals. Each probe extended a different distance into the boundary layer. The probes were constructed of stainless-steel tubing (0.89 mm o.d., 0.61 mm i.d.) and the nose of each probe extended 8 probe diameters upstream from the probe stem. A pressure tap on the surface of the model just upstream of the probe tips was used to measure the static pressure, which was assumed to be constant across the boundary layer.

The surface static pressures on the model were measured at ten axial locations upstream of the base. In addition, six static taps located on the blunt base were used to monitor the pressure at different radial distances from the model centerline. All the static taps were 0.762 mm in diam. The leads

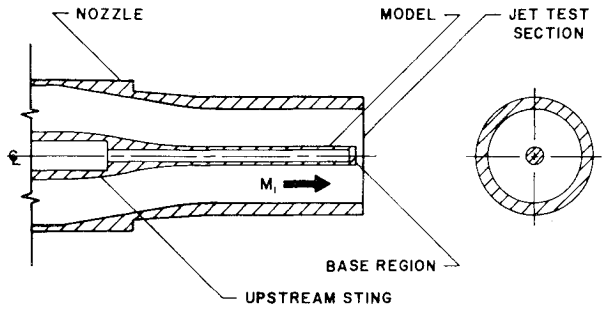

Fig. 3 RANT II schematic.

from these taps were brought outside the tunnel through the hollow centerbody.

Total and static pressures on the near-wake centerline were measured by extending either a pitot probe or a static probe from the blunt base through a hole in the center of the base. Both probes consisted of a straight piece of stainless-steel tubing (0.89 mm o.d., 0.61 mm i.d.). The tip of the pitot probe was open and rounded, while the static probe had a tip which was plugged and rounded. The static probe had an orifice 0.56 mm in diameter located on the side wall 0.60 mm from the tip. The location of both probes was changed by manually sliding them in or out of the base. The position of each was measured with a precision scale readable to 0.25 mm. During this portion of the investigation, the base pressure was measured to insure that the probes did not influence the basic flow. No change in base pressure was observed during the centerline surveys.

Throughout the investigation, the tunnel total pressure was monitored using a Kiel probe located in the tunnel plenum chamber. The signal sensed by the probe was measured with a Statham ±172 kPa gage transducer and an X-Y recorder. Plots of total pressure with time showed that it was constant during the test portion of each experimental run. The tunnel total temperature was measured with a copper-constantan thermocouple located in the tunnel plenum chamber and an X-Y recorder.

The pressure signals from all the pressure taps and probes were read out on manometer banks which were filled with either mercury or water. The manometers were readable to 0.13 cm of manometer fluid. Solenoid values located in the pressure leads protected the manometers from transients during tunnel start-up and trapped the signal just before shutdown so that readings could be made carefully after each test. The duration of each test run provided more than adequate time for the instruments to respond.

Test conditions for this investigation included: 1) the entire subsonic Mach number range, 2) Reynolds numbers from 0.1×10^7 to 3.1×10^7/m, 3) stagnation pressures from just above atmospheric pressure to 206 kPa absolute, and 4) stagnation temperatures of 283 K ± 11 K. Velocity profiles of the boundary layer approaching the blunt base showed that it was turbulent and fully developed for all approach Mach numbers.

Results

The development of the near-wake is dependent upon the flow conditions approaching the separation point. For this reason, it was necessary to determine the boundary-layer parameters on the model upstream of the blunt base.

The total and static pressure data from the boundary-layer model were reduced to velocity profiles by assuming constant static pressure across the boundary layer and isoenergetic flow for the tunnel. The velocity profiles were corrected for errors due to shear flow and wall proximity, as suggested by MacMillan.[23] Each velocity profile, especially those nearer the blunt base, exhibited a maximum velocity at the outer edge of the boundary layer. This maximum velocity was

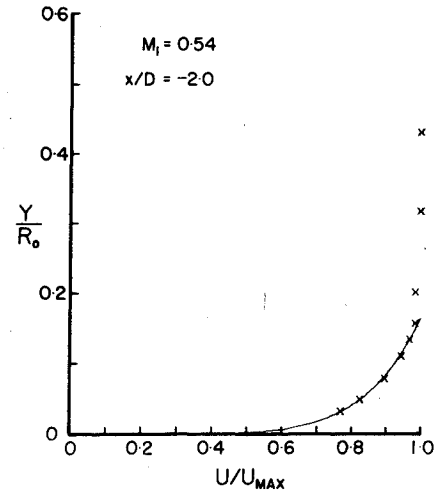

Fig. 4 Typical boundary layer velocity profile.

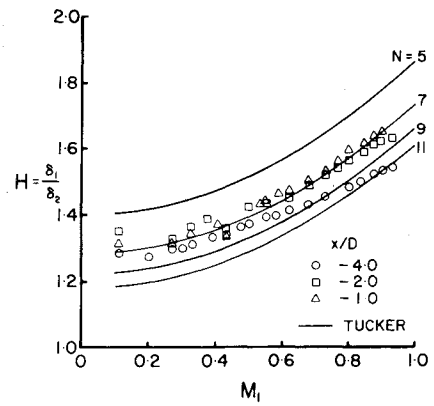

Fig. 5 Boundary layer shape factor vs Mach number.

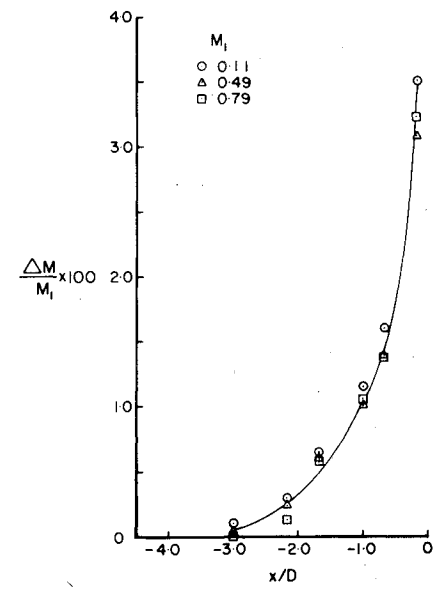

Fig. 6 Upstream influence of near-wake.

greater than the local freestream velocity. This velocity overshoot is due to the influence of the separation process at the blunt base on the subsonic approach flow. This upstream influence of the blunt base will be discussed in detail later in the paper. The velocity data were normalized with respect to the maximum velocity in each profile and plotted against vertical distance from the wall. Least-square curve fit procedures were used to obtain analytical expressions for the velocity profiles. These expressions were of a power law form. The power law exponent N was determined by the least-squares curve fit. In addition, rather than defining the boundary-layer thickness δ in the usual manner as the distance from the model surface at which the velocity in the boundary layer obtained some arbitrary percentage of the freestream velocity, the boundary-layer thickness was also determined by the best fit of the power law expression to the data. Thus, the boundary-layer thickness was defined as the distance from the model surface at which the power law expression for the normalized velocity was equal to 1.0. Figure 4 shows typical boundary-layer data and the best fitting power law. It should be noted that in Fig. 4 the power law was fit to the data points in the boundary layer. The three points furthest from the wall in Fig. 4 are in the freestream rather than the boundary layer.

Values for the displacement thickness and momentum thickness of each velocity profile were determined by numerically integrating the analytical expressions. The standard definitions of these parameters for axisymmetric flow were used for the integrations. The results of the analysis showed that the profiles of all three axial locations could be adequately represented as power laws for all Mach numbers tested. The power law exponent N was found to be between 5.5 and 9.5 for all cases, indicating that the boundary layer was turbulent and fully developed.

It is impossible to list the values of the boundary-layer parameters at all locations for every Mach number tested. However, Table 1 gives some representative values which show the order of magnitude of the boundary-layer parameters at the three locations for all the Mach numbers tested.

In general, the boundary layer thickness δ, displacement thickness δ_1, and momentum thickness δ_2 increased as the boundary layer approached the base. These three parameters decreased with increasing Mach number at all three axial locations. Figure 5 shows the shape factor H as a function of Mach number. The shape factor at all three axial locations increased with Mach number, in agreement with the theoretical calculations of Tucker[24] as shown in Fig. 5.

Table 1 Boundary layer parameters, $M_I = 0.54$

X/D	δ/R_0	δ_1/R_0	δ_2/R_0
−4.0	0.420	0.060	0.045
−2.0	0.425	0.070	0.048
−1.0	0.430	0.075	0.052

As previously mentioned, the separation process at the blunt base was found to have an influence on the subsonic flow approaching the base. This phenomenon has been observed by other investigators.[7,15,21] The presence of the blunt base resulted in a local acceleration of the flow along the model wall. This influence was found to extend 3 model diameters upstream of the base. Figure 6 shows the percentage change in the maximum local Mach number along the model wall for various freestream Mach numbers. In all cases, an increase in local Mach number of between 3.0% and 4.0% was found at $x/D = -0.167$. The location at which this acceleration started was approximately 3 model diameters upstream of the base at low Mach numbers. As the freestream Mach number increased, this point moved toward the base. Thus, the increase in local Mach number became more rapid at the higher freestream velocities.

Based on these results, the reference state for all the data obtained in this investigation was selected to be 3 model diameters upstream. For all cases, the local Mach number at this location was within 0.1% of the freestream Mach number.

A complete survey of the pressure acting on the blunt base was made. Measurements were made at the following radial

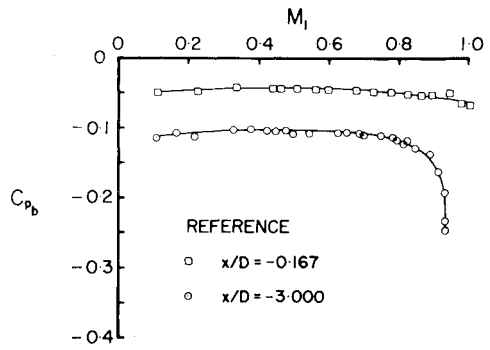

Fig. 7 Base pressure coefficient vs Mach number.

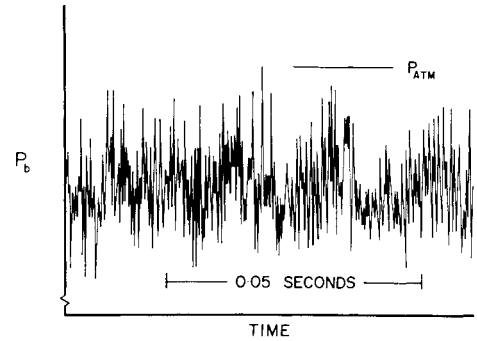

Fig. 8 Typical base pressure fluctuations.

locations on the blunt base: $r/R_0 = 0$, 0.167, 0.333, 0.500, 0.667, and 0.833. The base pressure was found to be a weak function of radial location at all Mach numbers. The maximum variation was approximately $\pm 5\%$ of the centerline base pressure. Figure 7 shows the base pressure coefficient, referenced to the flow conditions 3 diameters upstream of the base, as a function of Mach number. It can be seen that the base pressure coefficient has a relatively constant value of -0.11 for Mach numbers between 0.0 and 0.8. It should be noted that there was a very slight increase in the base pressure in the mid Mach number range and that a maximum value was achieved at Mach numbers between 0.4 and 0.6. At Mach numbers above 0.8, the base pressure begins to fall rapidly as sonic velocity is approached. These data provide a set of consistent base pressure results for a single simple geometry free of support interference and obtained in one test facility. These data are well within the range of the data shown in Fig. 2. It should be remembered that the data in Fig. 2 have been obtained in many facilities for a wide range of geometries and various approach flow conditions.

As discussed earlier, the separation process at the blunt base has an effect on the upstream approach flow. Many investigators use the static pressure on the model wall a short distance upstream of the base as a reference pressure, and claim that this pressure is equal to the freestream static pressure. This investigation and others have shown that this is not true. If the reference condition is located sufficiently close to the base, so as to be in the region of upstream influence, misleading results and trends can be obtained. Figure 7 shows the base pressure coefficients from this investigation plotted against Mach number using two different reference locations. In one case, the reference state is 3 model diameters upstream of the base, which has been shown to be outside the region of upstream influence and equal to the freestream condition. The second curve in Fig. 7 shows the same base pressure data referenced to the flow state just upstream of the base, which is within the region of upstream influence of the base. It can easily be seen that the use of this second reference state not only results in a magnitude difference, but completely hides the drop in base pressure which occurs at near-sonic speeds. Thus, when computing the base pressure from a set of pressure coefficients, particular attention must be given to the reference state of the coefficients. Since, in general, the freestream conditions for a particular problem are known or specified, it is desirable to use coefficients which have been referenced to a flow state, which is outside the region of upstream influence of the base and equal to the freestream state.

The base pressure results presented thus far have been time-averaged. An attempt was made to measure the fluctuating component of the base pressure using a base-mounted pressure transducer with a frequency response of 70,000 Hz and a light beam oscillograph. Although the method was too crude to obtain quantitative results, some qualitative remarks are in order. Figure 8 shows a trace of the output signal from

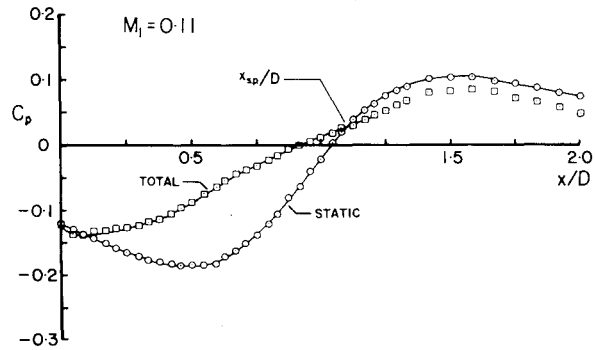

Fig. 9 Near-wake centerline pressure distributions.

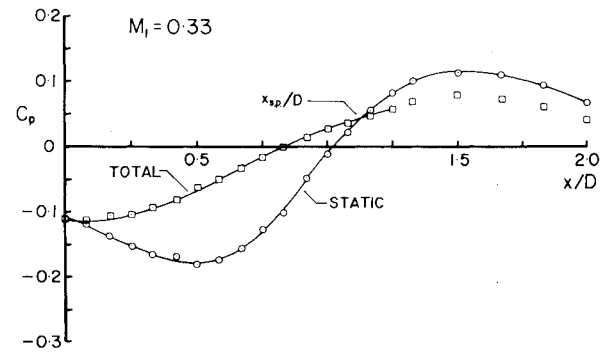

Fig. 10 Near-wake centerline pressure distributions.

the transducer. This plot is typical of the data obtained at all Mach numbers. It is quite evident that the base pressure is not constant with time, but rather exhibits rapid fluctuations about a mean value. The fluctuations were of the same order of magnitude as the difference between the time-averaged base pressure and the ambient atmospheric pressure. The magnitude of the fluctuations increased with increasing Mach number. The frequencies of the fluctuations decreased with increasing Mach number from approximately 2000 Hz at the low Mach numbers to about 1000 Hz at the high Mach numbers.

The total and static pressures on the near-wake centerline are shown in Figs. 9-14 for six different approach Mach numbers.[1] In each case, the static pressure decreases from the base pressure to a minimum value. The exact location and extent of the region over which this minimum value occurs depends on the Mach number of the approach flow. In general, the minimum value occurred between 0.5 and 0.7 model diameters downstream of the base. At the lower Mach numbers, the static pressure is essentially constant at the minimum value over the very small region behind the base. At the higher Mach numbers, this region becomes larger and

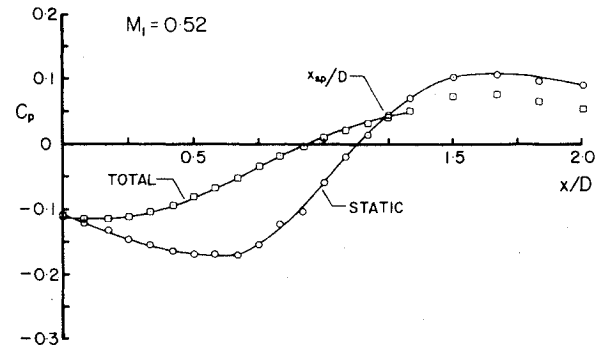

Fig. 11 Near-wake centerline pressure distributions.

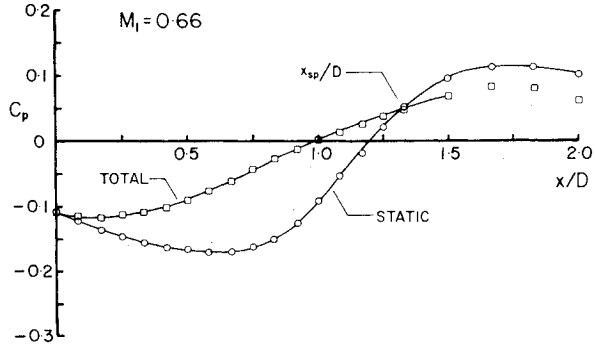

Fig. 12 Near-wake centerline pressure distributions.

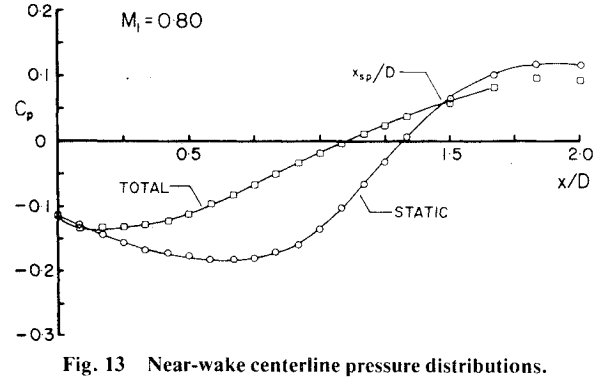

Fig. 13 Near-wake centerline pressure distributions.

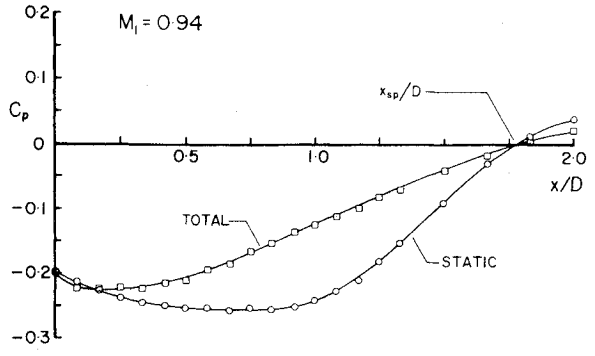

Fig. 14 Near-wake centerline pressure distributions.

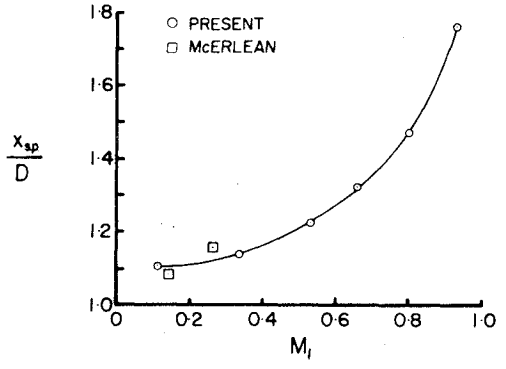

Fig. 15 Rear stagnation point location vs Mach number.

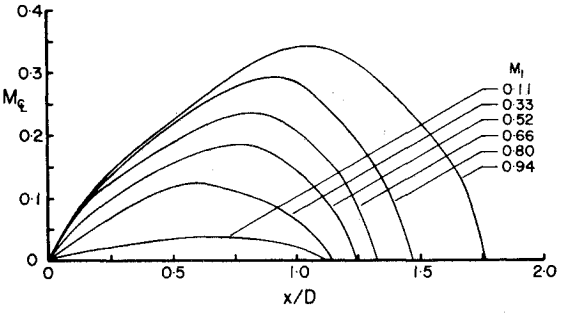

Fig. 16 Near-wake centerline Mach number distributions.

approaches 0.5 model diameters in length. After the region of approximately constant pressure, the static pressure increases to a maximum value that is greater than the upstream reference pressure. This maximum pressure occurs between 1.5 and 2.0 model diameters downstream of the base, depending on the approach Mach number. Although not shown in the plots, the static pressure for all six cases was essentially equal to the ambient atmospheric pressure at 4 model diameters downstream of the base.

For all cases, the total pressure at first decreased slightly from the base pressure. This slight decrease was followed by a steady increase to a value approximately equal to the upstream reference pressure as the rear stagnation point is approached. It should be noted that data points from the total pressure probe are shown beyond the rear stagnation point in each plot. However, since the flow did not impinge on the probe orifice, these data points do not represent the total pressure on the near-wake centerline.

The time-averaged rear stagnation point was located from the plots of centerline total and static pressures. The point on each plot where the total and static pressures are equal is the time-averaged rear stagnation point. At this point, the average centerline velocity is zero. Figure 15 shows the location of the rear stagnation point as a function of Mach number. It can be seen that as Mach number increased, the rear stagnation point moved downstream. For all subsonic Mach numbers, the rear stagation point was located between 1 and 2 model diameters downstream of the base. The present results are in agreement with those of McErlean[21] for the incompressible case.

It is interesting to note that there appears to be a second point on each plot where the total pressure and static pressure are equal. These points, which are very near the base, indicate another stagnation point and the presence of a secondary separated region. This phenomenon has been observed and measured in two-dimensional separated flows.[25]

The near-wake centerline velocity distributions were computed from the total and static pressure surveys. For all cases, the maximum centerline velocity was between 35% and 40% of the freestream velocity. The location of the maximum velocity varied from approximately 0.6 model diameters downstream of the base for the incompressible case to about 1.0 model diameters downstream for the near-sonic case. Figure 16 shows the centerline Mach number distributions for six approach Mach numbers. Clearly, the recirculation region is not a relatively stagnant region, as suggested by some investigators.

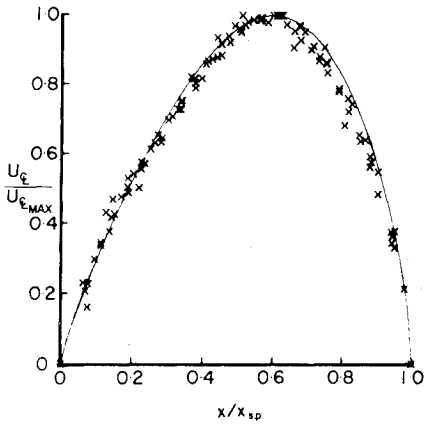

Fig. 17 Similarity of near-wake centerline velocity distribution.

An attempt to find a similarity expression for the near-wake centerline velocity distribution was made. When the velocity data were normalized with respect to the maximum centerline velocity and plotted against distance to the rear stagnation point, an excellent correlation was obtained for all approach Mach numbers. A curve was fit to the data. The curve was of the form

$$U_c/U_{c_{max}} = \sin^m[\pi(x/x_{s.p.})^n] \quad (1)$$

where $n = 1.356915$ and $m = 0.612949$.

The data showed that the maximum centerline velocity occurred at a location approximately 0.6 of the distance to the rear stagnation point. Therefore, the value of n was determined such that $U_c/U_{c_{max}} = 1.0$ at $x/x_{s.p.} = 0.6$. The value of m was determined from the data by a least-squares method. The data and the curve fit are shown in Fig. 17.

Conclusions

The turbulent near-wake of a cylindrical blunt-based body has been investigated. The experiments were conducted in a special wind tunnel. Model support interference in this facility has been eliminated by incorporating an upstream sting into the nozzle design. The experiments were conducted over the entire subsonic Mach number range and at Reynolds numbers between 0.1×10^7 and 3.1×10^7/m. The following are the major conclusions of this study:

1) The influence of the near-wake extends at least 3 body diameters upstream of the base. The reference condition for normalizing near-wake data should be outside of this region of influence.

2) The local flow adjacent to the body accelerates as the blunt base is approached. The maximum local Mach number at $x/D = -0.167$ was 3-4% greater than the freestream Mach number.

3) The time-averaged base pressure coefficient was constant at a value of -0.11 for Mach numbers between 0.0 and 0.8, with a very slight increase noted between Mach numbers 0.4 and 0.6. A rapid drop in base pressure was observed above a Mach number of 0.8 as near-sonic speeds were approached.

4) The instantaneous base pressure was found to fluctuate about a mean value. The frequency of the fluctuations was found to decrease with increasing Mach number, while the magnitude of the fluctuations increased. Frequencies between 1000 and 2000 Hz were observed. Magnitudes were significant.

5) Significant total and static pressure gradients existed on the near-wake centerline. The static pressure did not become equal to the freestream static pressure until $x/D > 4.0$.

6) The size and location of the constant pressure mixing region was found to depend on Mach number. In general, this region started between $x/D = 0.4$ and 0.5. Its length increased with increasing Mach number.

7) The rear stagnation point was located between 1 and 2 model diameters downstream of the base. The length of the recirculation region was relatively insensitive to changes in Mach number for incompressible flow ($M < 0.3$). As Mach number increased ($M > 0.3$), the rear stagnation point moved downstream. The static pressure at the rear stagnation point was slightly greater than the freestream static pressure.

8) The maximum velocity on the near-wake centerline was 35-40% of the freestream velocity and was found to occur at $x/x_{s.p.} = 0.6$ for all Mach numbers.

9) The centerline velocity distributions in the recirculation region exhibit similarity for all approach Mach numbers and can be represented by a simple expression derived from a correlation of the data.

Acknowledgment

The authors gratefully acknowledge the Emil Buehler Fund and Rutgers University for the support of this research.

References

[1] Stoney, W. D., Jr., "Collection of Zero-Lift Drag Data on Bodies of Revolution from Free-Flight Investigations," NACA TN 4201, 1957.

[2] Eldred, K. M., "Base Pressure Fluctuations," *The Journal of the Acoustical Society of America*, Vol. 33, Jan. 1961, pp. 59-63.

[3] Rossiter, J. E. and Kurn, A. G., "Wind Tunnel Measurements of the Effect of a Jet on the Time Average and Unsteady Pressures on the Base of a Bluff Afterbody," RAE TR-65187, Aug. 1965.

[4] Butsko, J. E., Carter, W. V., and Herman, W., "Development of Subsonic Base Pressure Prediction Methods," AFFDL-TR-65-157, Vols. I & II, Sept. 1965.

[5] Mair, W. A., "The Effect of a Rear Mounted Disc on the Drag of a Blunt Based Body of Revolution," *The Aeronautical Quarterly*, Vol. 16, Nov. 1965, pp. 350-360.

[6] Calvert, J. R., "Experiments on Low Speed Flow Past Cones," *Journal of Fluid Mechanics*, Vol. 27, Part 2, Jan. 1966, pp. 273-289.

[7] Kurn, A. G., "Drag Measurements on a Series of Afterbodies at Transonic Speeds Showing the Effects of Sting Interference," RAE TR-66298, Sept. 1966; also, Aeronautical Research Council C. P. No. 984, 1968.

[8] Greenwood, G. H., "Measurement of Drag, Base Pressure and Base Aerodynamic Heat Transfer Appropriate to 8.5 Degree Semi-Angle Sharp Cones in Free Flight at Mach Numbers from 0.8 to 3.8," RAE TR-66394, Dec. 1966.

[9] Slatten, T. R., "The Effect of Upstream Geometry on Axisymmetric Subsonic Base Flow," M.S. Thesis, Dept. of Mechanical Engineering, University of Washington, 1967.

[10] Vanwagenen, R., "A Study of Axially-Symmetric Subsonic Base Flow," Ph.D. Thesis, Dept. of Mechanical Engineering, University of Washington, 1968.

[11] Compton, W. G., III, "Effect on Base Drag of Recessing the Bases of Conical Afterbodies at Subsonic and Transonic Speeds," NASA TN D-4821, Oct. 1968.

[12] Oswandel, K. J., "Subsonic Axisymmetric Near-Wake Studies," M.S. Thesis, Mechanical Industrial, and Aerospace Engineering Department, Rutgers University, May 1969.

[13] Sykes, D. M., "Cylindrical and Boat-Tailed Afterbodies in Transonic Flow with Gas Injection," *AIAA Journal*, Vol. 8, March 1970, pp. 588-590.

[14] Mabey, D. G., "Some Measurements of Base Pressure Fluctuations at Subsonic and Supersonic Speeds," Aeronautical Research Council, C.P. No. 1204, Aug. 1970.

[15] Riddle, R. A., "An Experimental Investigation of a Subsonic Axisymmetric Open Wake," M.S. Thesis, Mechanical, Industrial, and Aerospace Engineering Dept., Rutgers University, June 1971.

[16] Koh, J. C. Y., "A New Wind Tunnel Technique for Providing Simulation of Flight Base Flow," *Journal of Spacecraft and Rockets*, Vol. 8, Oct. 1971, pp. 1095-1096.

[17] Usry, J. W. and Wallace, J. W., "Drag of a Supercritical Body of Revolution in Free Flight at Transonic Speeds and Comparison with Wind Tunnel Data," NASA TN D-6850, Dec. 1971.

[18] Rom, J., Victor, M., Reichenberg, M., and Salomon, M., "Wind Tunnel Measurements of the Base Pressure on an Axially Symmetric Model in Subsonic, Transonic, and Supersonic Speeds at High Reynolds Numbers," Technion-Israel Institute of Technology, T.A.E. Rept. No. 134, Sept. 1972.

[19] Yajnik, K. S., Kangovi, S., and Seshodri, S. M., "Effect of Sting on Base Pressure in High Subsonic and Transonic Speeds," Paper presented at Commonwealth Aeronautical Advisorty Research Council (CAACR), Bangalore, India, Dec. 1972.

[20] Merz, R. A., "The Turbulent Near-Wake of an Axisymmetric Blunt Based Body at Subsonic Speeds," Ph.D. Thesis, Mechanical, Industrial, and Aerospace Engineering Department, Rutgers University, May 1975.

[21] McErlean, D. P., "The Near-Wake of a Blunt Based Axisymmetric Body at Mach .14," Ph.D. Thesis, Mechanical, Industrial, and Aerospace Engineering Department, Rutgers University, Jan. 1970.

[22] Halleen, R. W., "A Literature Review on Subsonic Free Turbulent Shear Flow," Rept. MD-11, Stanford Universtiy, AD 606758, April 1964.

[23] MacMillan, F. A., "Experiments on Pitot-Tubes in Shear Flow," Repts. and Memo. No. 3028, Feb. 1956.

[24] Tucker, M., "Approximate Calculations of Turbulent Boundary Layer Development in Compressible Flow," NACA TN-2337, April 1951.

[25] DeRossett, T. A., "An Experimental Investigation of Subsonic Steady and Oscillating Flow over an Axisymmetric Backstep," Ph.D. Thesis, Mechanical, Industrial, and Aerospace Engineering Dept., Rutgers University, May 1973.